Creating a database of helicopter main rotor acoustics for validation of CFD methods

Pakhov, V., Stepanov, R.*, Bozhenko, A.*, Batrakov, A.*, Kusyumov, A.*, Mikhailov, S.* and Barakos, G.***
**Kazan National Research Technical University n.a. A.N. Tupolev (KNRTU-KAI), Kazan, Russia*
VVPakhov@kai.ru
*** Professor, School of Engineering, James Watt South Bld., School of Engineering, University of Glasgow, RAeS Member*
George.barakos@glasgow.ac.uk

Abstract

The work presents recent experiments at the Kazan National Technical University (KNRTU-KAI), related to helicopter acoustics. The objective is to provide a database of near-field experimental data suitable for CFD validation. The obtained set of data corresponds to a Mach-scaled rotor of known planform. An advantage of the current dataset is that direct near-field acoustic data is made available and this allows easy and direct comparisons with CFD predictions, without the need to use far-field aeroacoustic methods.

1. Introduction

Reduction of helicopter rotor noise is an important objective for design engineers aiming to achieve certification of new rotorcraft that are compliant with the stringent noise regulations for operations from airports and inhabited areas. Rotor noise contains broadband and discrete noise components. The broadband noise includes non-deterministic loading noise, which includes blade self-noise, blade-to-wake interaction noise and turbulent ingestion noise. The discrete-frequency noise consists of deterministic components of thickness, loading and high-speed impulsive noise tones that are dominant throughout the flight envelope of the helicopter [1].

Thickness noise occurs because of the displacement of the air by the blade. It is mainly determined by the airfoil thickness and rotor speed [2]. It propagates mainly in the rotor plane in front of the upcoming blade. This type of noise occurs mostly at the tip of the rotor due to the high tangential speeds of the blade sections. The thickness noise is the dominant noise component for an observer on the rotor plane, especially for hovering rotors.

The experience gained from the HART program [3-5] has shown that a key parameter for noise simulation is the successful wake simulation, especially if BVI noise is considered. To this end, prescribed wake theory [6] and free wake simulation [3,7,8] have been successfully used in the past.

At the moment, the access to all experimental data of near-field aeroacoustic measurements is limited. However, all data, presented in this paper, is planned to be made publicly available, including the blade shape geometry and all measurements [9].

.

2. Experimental setup and experiment conditions

2.1Wind tunnel

The experiments were conducted in the acoustic chamber of the T-1K wind tunnel (WT) at KNRTU-KAI (Kazan, Russia).To perform the acoustic and aerodynamic experiments modifications were necessary, including the addition of ceiling and side walls, running between the jet and diffuser.

The retractable walls include Helmholtz resonators for absorbing acoustic noise of low frequencies coupled with pyramid shape melamine foam material for absorbing acoustic noise of higher frequencies. The Helmholtz resonators were designed to enable aero-acoustic rotor measurements of the rotor rig at lower frequencies (See Figure 1 for an overview of the test section).

Main object of experiments described in this work is a mach-scaled rotor. Such rotors have high rotational speeds, and tend to generate acoustic pressure in much higher frequencies compared to full size helicopters. Therefore, the melamin-based acoustic absorbing material was selected to satisfy those requirements. A scheme of the wind tunnel and acoustic chamber is sown on Figure 1.

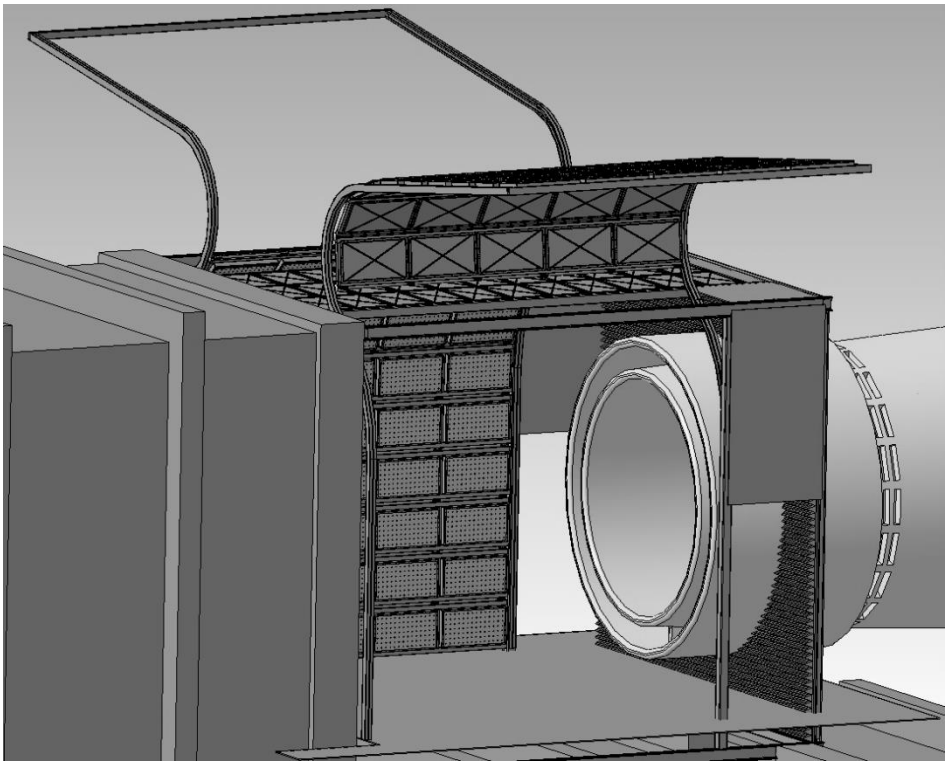

Figure 1: Wind tunnel and acoustic camera schematic.

2.2Rotor rig

For this work, the angular speed of the rotor was set to 900 rpm. The collective pitch angle at 75% of blade radius $\theta_{.75}$ was set to +8°. All tests were performed in hover mode, i.e. with no free stream velocity. The rotor radius was $R = 0.820\ m$. In this work, however, all the distances will be presented in terms of relative radius $\bar{r} = r/R = 1.2$, where r is a horizontal distance from the rotor's axis of rotation, and the relative distance $\bar{y} = y/R$, where y is a vertical distance from the rotor plane (see Figure 2). Rotor rig had four blades of known geometry with parabolic tips. (see Figure 3)

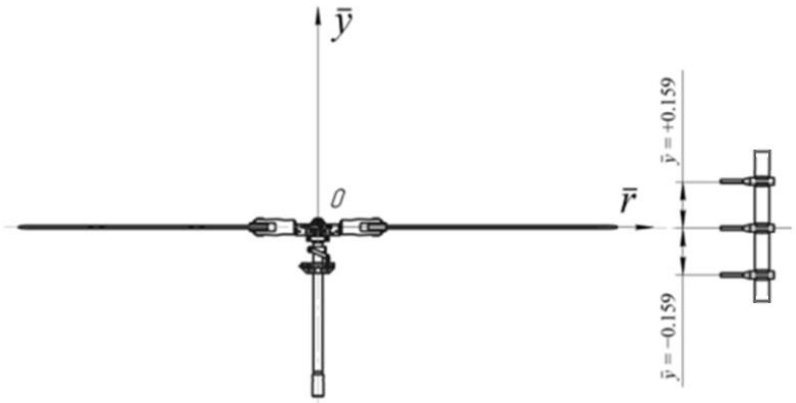

Figure 2: Placement of the microphones during the experiments. The linear array is shown adjacent to the rotor.

2.3Data acquisition and analysis

The measurements were taken with DBX RTA-M microphones coupled with Panasonic WM-61A cartridges. An NI-PXI 4496 ADC card, supporting sampling rates of up to 204kS/s with 24-bit analogue-to-digital conversion, was used. This setup allowed recording signals from the microphones simultaneously.
The microphone placement is shown on Figure 2, with the microphone array positioned at a relative radius $\bar{r} = 1.2$.

3. CFD setup and conditions

Numerical simulations of the flow around the rotor model for hover mode were based on the RANS approach with the k-ω turbulence model, and carried out with HMB CFD-code. The flow around the isolated rotor in hover mode has a periodic structure. For this reason, a computational domain was constructed for one blade only (Figure 3). A multiblock grid was created using the ICEM Hexa™ tool and contained 4.4 million points.
The near field sound generation at any considered point is determined by the fluctuation of the static pressure induced by the rotation of the rotor. The grid consisted of 172 blocks and 4.4 millions of points with a careful arrangement to capture the loading of the blade and provide good resolution of the wake. The grid was constructed using previous experience with similar configurations [10], and while it was coarse, it captured the main flow features with relatively good accuracy.

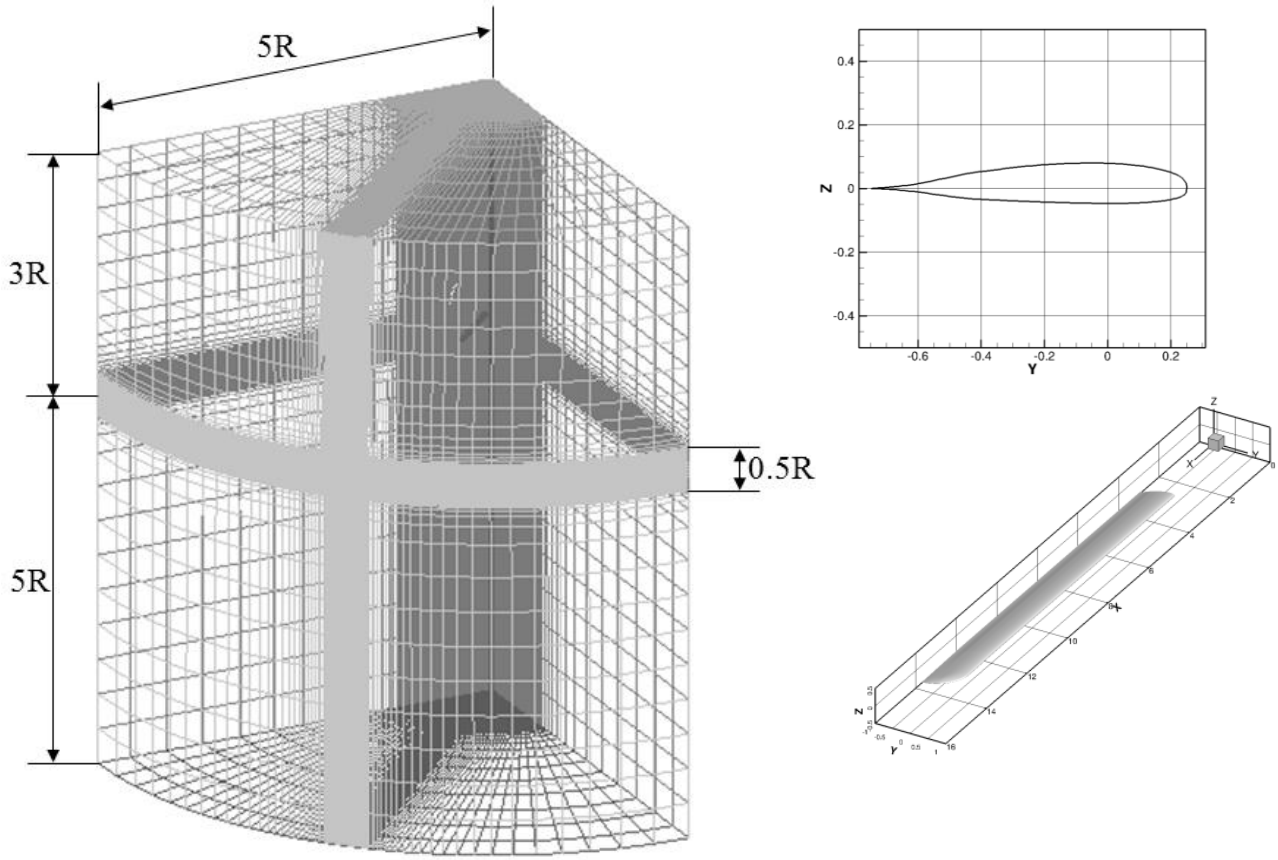

Figure 3: Computational grid for one blade of the rotor.

4. Results and discussion.

Figure 4 presents experimental and CFD results of wake boundaries in hover flight obtained at KNRTU-KAI. The flow visualization was performed using a Dantec PIV system with a Nd:YAG laser. The vortices were identified using *Q*-criterion for a 2D case, defined as connected spatial regions, where the Euclidean norm of the vorticity tensor dominates the rate of the strain tensor, i.e. when the $Q > 0$ condition is satisfied [11].

The position of each vortex, obtained in the experiment for multiple frames, is shown by dots in Figure 4, which are then approximated with a polynomial line. The CFD results are then added to Figure 4, which show good agreement with the experiment.

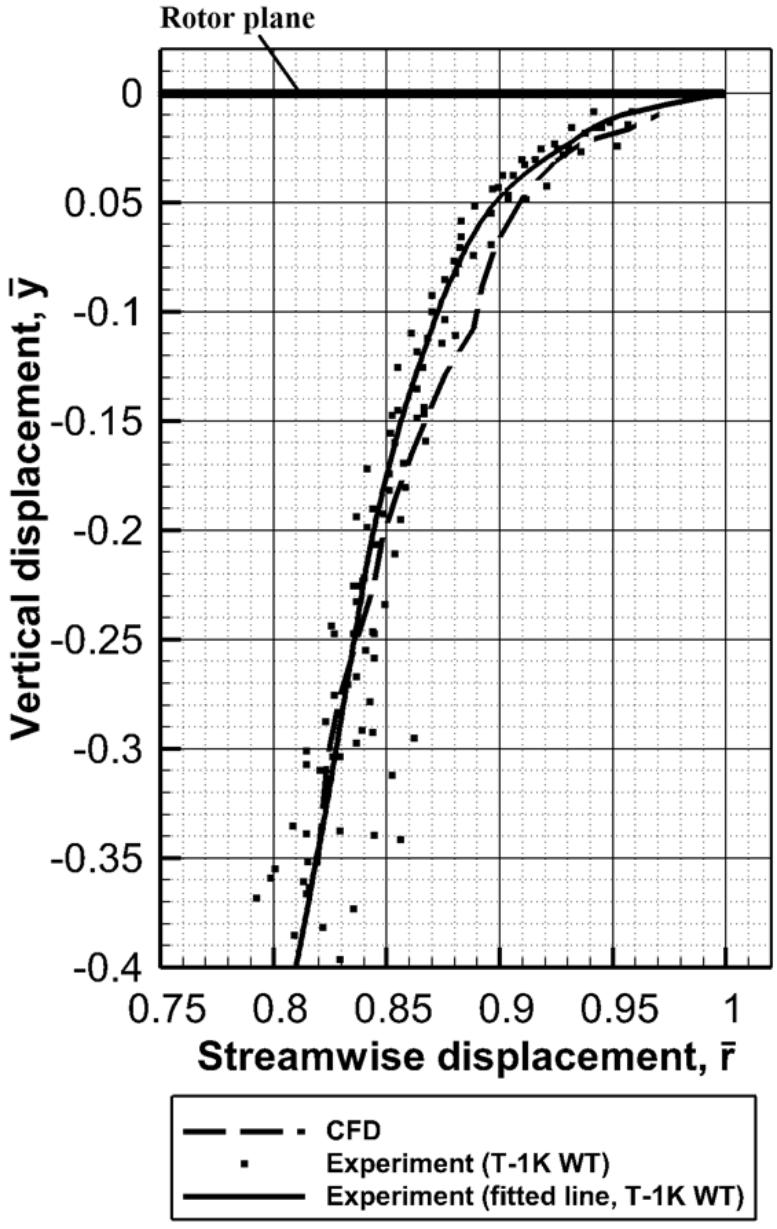

Figure 4:Comparison CFD with experimental results of tip vortex coordinates for the hover flight

Figure 5 shows the noise level distribution around the rotor rig, which was operating in hover mode at a collective pitch angle of 8 degrees, at different distances from rotor ($\bar{r}$ =1.2 to 2.1 in steps of 0.1). The vertical asymmetry of the peak sound level is believed to be caused by coning angle of the rotor. Figure 6 presents the comparison between CFD and experimental exponential sound level at the distance $\bar{r}$ =1.2.

Comparison of sound pressure levels (SPL) in the temporal domain for experimental results and CFD computations are shown in Figures 7-9. Each microphone position is defined by relative distances $\bar{r}$ =1.2 and $\bar{y}$ with respect to the rotor plane. In order to show the distribution of the acoustic pressure, the first five periods of the experimental data, taken from the same microphone, are shown (Exp-1 denotes the first period, Exp-2 the second period, etc.). The results were then compared to the CFD data (red line). The peaks at time instances t_1,t_2,t_3 andt_4 are marked in Figures 7-9by vertical dashed lines. The time span on these figures corresponds to a full revolution of the rotor.

The comparison of the experimental and CFD data also show that these results are in a good agreement with each other. However, contrary to experiments, where the coning angle of the rotor changed due to operating conditions ($\beta_0 \neq 0$), the coning angle for the CFD simulations was set to zero ($\beta_0 = 0$).

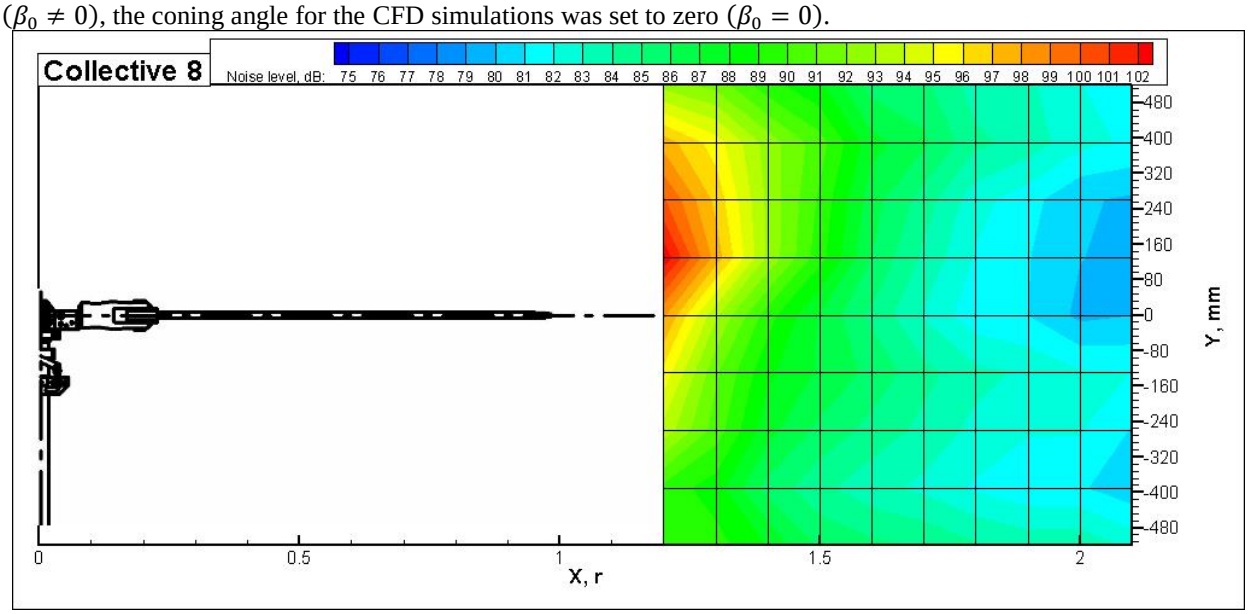

Figure 5:Exponential sound level values. Experimental results. $C_T = 0.01,\ \theta_0 = 8°, M_{tip} = 0.23$.

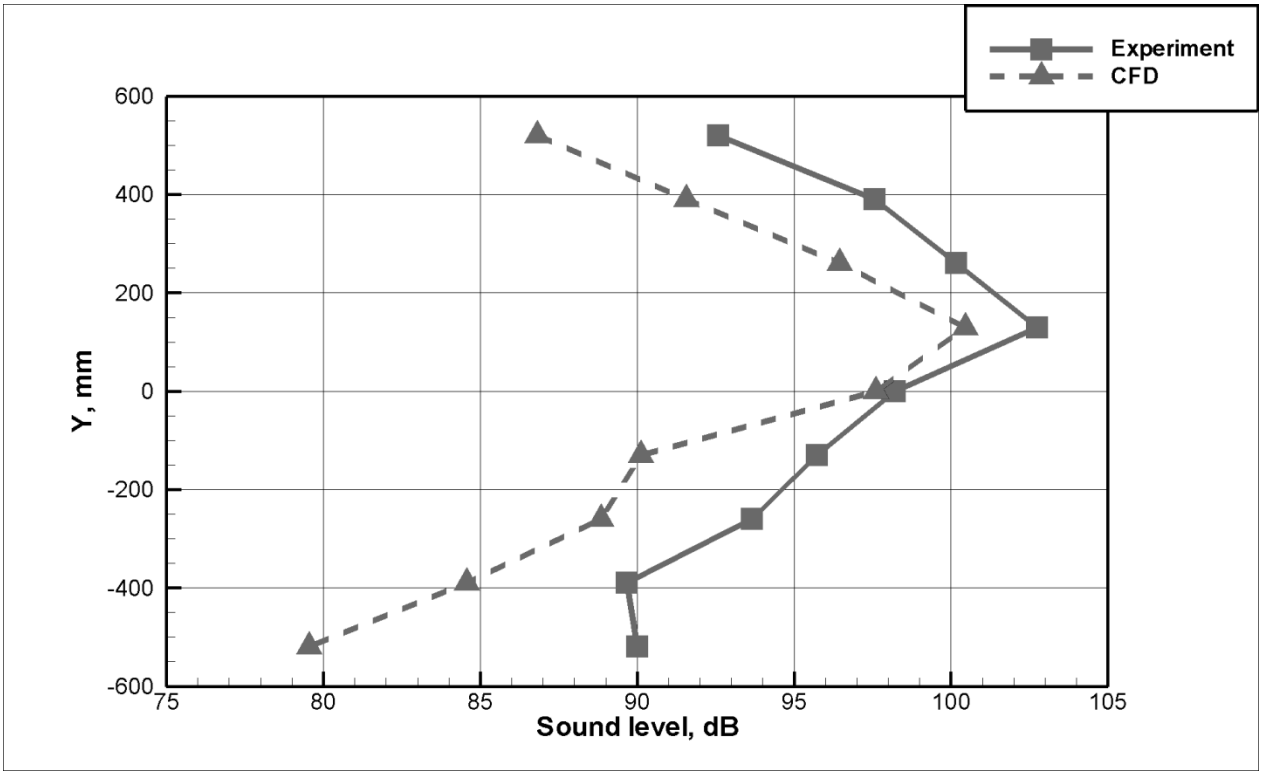

Figure 6:Comparison of CFD and experimental results. $C_T = 0.01,\ \theta_0 = 8°, M_{tip} = 0.23$.

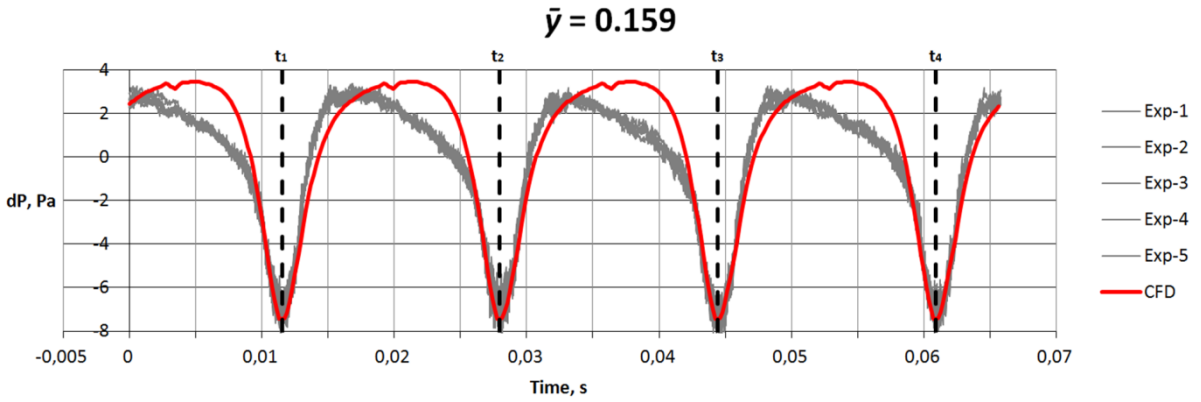

Figure 7. Comparison of the first five periods (Exp-1 to Exp-5) of the experimental measurements and CFD results for vertical distance from the rotor plane $\bar{y} = 0159$. The peaks at $t_1 = 0.01152\ s$,$t_2 = 0.02798\ s$,$t_3 = 0.04444\ s$ and$t_4 = 0.06090\ s$ are shown with dashed vertical lines.

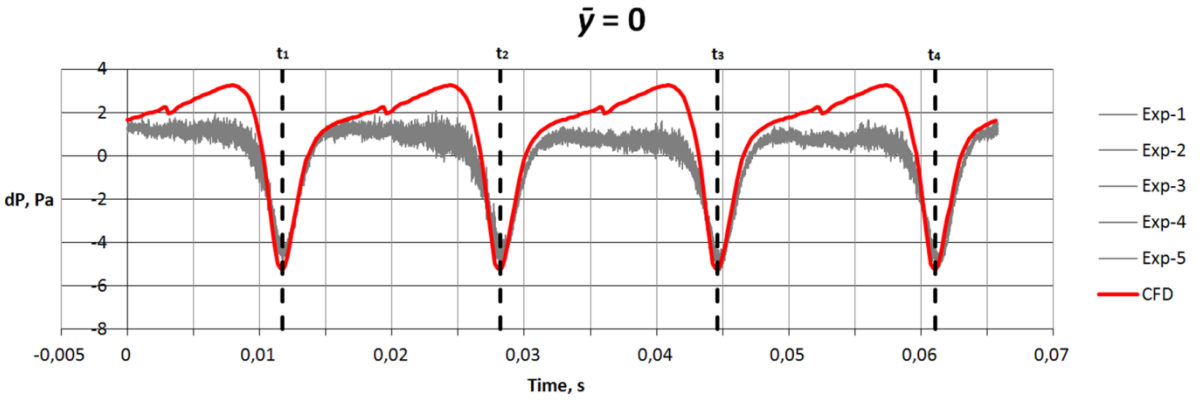

Figure 8. Comparison of the first five periods (Exp-1 to Exp-5) of the experimental measurements and CFD results for vertical distance from the rotor plane $\bar{y} = 0$. The peaks at $t_1 = 0.01170\ s$,$t_2 = 0.02816\ s$,$t_3 = 0.04462\ s$ and$t_4 = 0.06108\ s$ are shown with dashed vertical lines.

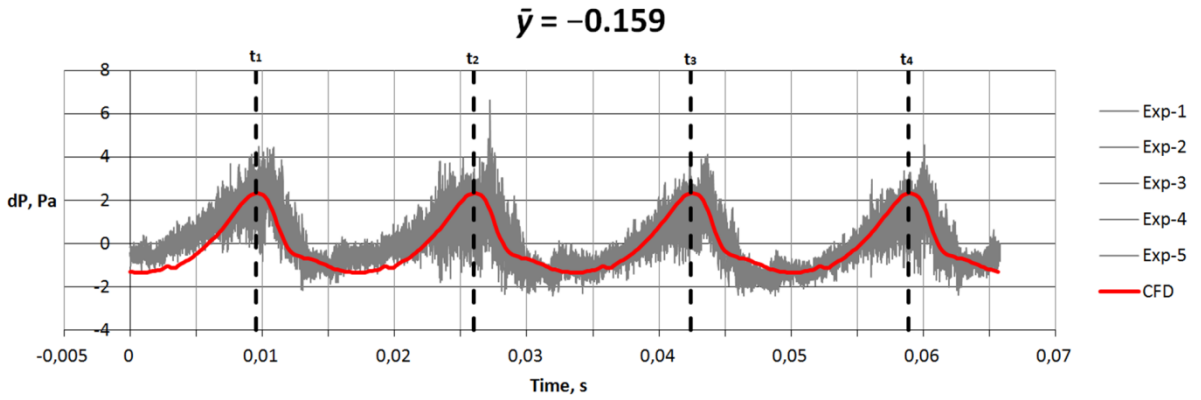

Figure 9. Comparison of the first five periods (Exp-1 to Exp-5) of the experimental measurements and CFD results for vertical distance from the rotor plane $\bar{y} = -0.159$. The peaks at $t_1 = 0.00951\ s$,$t_2 = 0.02597\ s$,$t_3 = 0.04243\ s$ and$t_4 = 0.05888\ s$ are shown with dashed vertical lines.

5. Conclusions.

The work presented experimental results obtained using a near-field linear array for a model-scale rotor in hover. The array was placed at 1.2R distance from the rotor. The comparison of experimental data with the CFD simulation results of acoustic pressure fluctuations in temporal domain showed good agreement. The CFD simulations were based on RANS solutions obtained using the in-house HMB code. So far, the following conclusions can be drawn:
1. Experimental data can be used for initial validation of CFD solvers, which are easy to run and economic in CPU time.
2. The data appears to be accurate and agree with theoretical estimates and preliminary CFD-results.
Future studies will be aimed at forward flight with focus on BVI and HIS noise studies, using near-field microphone arrays. Future simulations are also to be performed for validating the HMB solver.

6. Acknowledgements

This work was supported by the grant ‘Numerical and physical modelling of aerodynamic and aeroacoustic characteristics of rotor systems of future concept aircarft' (No. 9.1577.2017/ P Ch) of the Ministry of Education and Science of the Russian Federation.

References

[1] Schmitz FH, Boxwell DA, Splettstoesser WR, Schultz KJ. Model-rotor high-speed impulsive noise: Full-scale comparisons and parametric variations. *Vertica*, 8(4), pp. 395-422, 1984.
[2] van der Wall BG, Burley CL, Yu Y., Hugues R, Pengel K, Beaumier P. The HART II test – measurement of helicopter wakes. *Aerospace Science and Technology*. Volume 8, Issue 4, June 2004, pp.273-284.
[3] Berend G. van der Wall, Casey L. Burley, Yung Yu, Hugues Richard, Kurt Pengel, Phillipe Beaumier, “The HART II test – measurement of helicopter wakes,” *Aerospace Science and Technology*. Volume 8, Issue 4, June 2004, pp.273-284. (doi:10.1016/j.ast.2004.01.001).
[4] P. Beaumier, P. Spiegel, Validation of ONERA prediction methods for blade-vortex interaction using HART results, in: *51st Annual Forum of the American Helicopter Society*, Fort Worth, TX, 1995.
[5] B.G. van der Wall, Vortex characteristics analysed from HART data, in: *23rd European Rotorcraft Forum*, Dresden, Germany, 1997.
[6] B.G. van der Wall, Simulation of HHC on helicopter rotor BVI noise emission using a prescribed wake method, in: *26th European Rotorcraft Forum*, The Hague, Netherlands, 2000.
[7] T.F. Brooks, D.D. Boyd, C.L. Burley, J.R. Jolly, Aeroelastic codes for rotor harmonic and BVI noise – CAMRAD.Mod1/HIRES, in: *2nd AIAA/CEAS Aeroacoustics Conference*, State College, PA, 1996.
[8] B.G. van der Wall, M. Roth, Free-wake analysis on massively parallel computers and validation with hart test data, in: *53rd Annual Forum of the American Helicopter Society*, Virginia Beach, VA, 1997.
[9] http://agd.kai.ru/
[10] Garipova LI, Batrakov AS, Kusyumov AN, Mikhailov SA, BarakosG.Aerodynamic and acoustic analysis of main rotor blade tip part for hover.*50h 3AF International Conference on Applied Aerodynamics*, 29-30 March – 01 April 2015, Toulouse - France. Pp. 1–6.
[11] Haller G. An objective definition of a vortex.*J. Fluid Mech.*, vol. 525, pp.1–26, 2005.DOI: 10.1017/S0022112004002526.